Hindawi
Journal of Nanomaterials
Volume 2022, Article ID 7155557, 8 pages
https://doi.org/10.1155/2022/7155557

Research Article

Organic Template-Free Synthesis of Mesoporous ZnO Microparticles by Sol-Gel Method and Low-Temperature Hydrothermal Treatment

B. Murguía,[1] **A. Medina**,[1] **S. Borjas**,[2] **E. Díaz**,[3] **and C. Aguilar**[4]

[1]*Instituto de Investigación en Metalurgia y Materiales, Universidad Michoacana de San Nicolás de Hidalgo, Morelia, Michoacán, Mexico*
[2]*Instituto de Física y Matemáticas, Universidad Michoacana de San Nicolás de Hidalgo, Morelia, Michoacán, Mexico*
[3]*Centro de Investigación en Química Aplicada, Saltillo, Coahuila, Mexico*
[4]*Departamento de Ingeniería Metalúrgica y Materiales, Universidad Técnica Federico Santa María, Valparaíso, Chile*

Correspondence should be addressed to A. Medina; ariosto.medina@umich.mx

Received 10 September 2021; Revised 8 February 2022; Accepted 4 April 2022; Published 30 April 2022

Academic Editor: Hiromasa Nishikiori

Mesoporous zinc oxide microparticles were synthesized by the sol-gel method, followed by hydrothermal treatment at three different temperatures (100°C, 120°C, and 140°C), confirming that the method is fast, simple, reproducible, and ecological. To carry out the synthesis of the samples, zinc acetate was used as a precursor and sodium hydroxide as a precipitating agent. From the results obtained, the sample that shows the highest mesoporosity was the one synthesized at a hydrothermal treatment temperature of 140°C, obtaining an average particle size of 5 μm and a pore diameter of 1.7 nm. The importance of the results obtained was that mesoporous xerogel microparticles were obtained without using any type of organic template.

1. Introduction

Mesoporous materials are quite useful and can be used in various areas of our life because they have a crystalline structure and physicochemical properties with the ability to adsorb and interact with ions, atoms, and molecules on their surface. Techniques and methods have been developed to synthesize mesoporous materials with a defined structure and morphologies [1–5]. However, the techniques developed so far are expensive, since they use surfactant molecular molds in solution, as well as ion block copolymers when it comes to Santa Barbara Amorphous (SBA), in addition to using temperatures above 150°C during hydrothermal treatment.

ZnO is considered nontoxic to living beings. It is a well-studied transparent wide band-gap semiconductor (E_g = 3.37 eV) with a large exciton binding energy (~60 meV) that presents potential applications in solar cells, antibacterial methods, sensing, photocatalysis and optical [6–13]. There is currently little information on the successful preparation of ZnO mesoporous microparticles without the use of some type of organic template.

This research explores the synthesis technique without using some type of organic template or block copolymer, using the sol-gel method with a hydrothermal treatment temperature lower than and equal to 140°C, which reduces the cost and energy used.

2. Materials and Methods

In general, two solutions were prepared; the first one was obtained by dissolving 0.02 mol of zinc acetate dihydrate in 18 mL of distilled water (S1). The second solution was obtained by dissolving 0.02 mol sodium hydroxide in 1.2 mol distilled water (S2). Later, the two solutions were mixed, S2 (approximately 0.05 mL/10 s) was added to S1, which was kept under constant stirring at 350 rpm at room temperature, while S2 was added.

Once S2 was added to S1, the xerogel obtained was stirred at 500 rpm for 30 min at room temperature. The molar ratio was (zinc acetate : NaOH : H_2O) = (1 : 1 : 120). Subsequently, the xerogel was subjected to hydrothermal treatment at three different temperatures of 100°C, 120°C, and 140°C for 24 h. The samples were identified as AZn100, AZn120, and AZn140, respectively. After hydrothermal treatment, the samples were washed with distilled water and centrifuged at 12,000 rpm for 5 min. Finally, the resulting ZnO powder microparticles were dried at 80°C for 24 h to then be ground in a mortar. It was necessary to calcine the powders at 560°C for 1 h to eliminate organic traces.

2.1. Characterization. X-ray diffraction analysis of the samples was performed using a Bruker D8 Advance X-ray diffractometer employing CuK_α radiation ($\lambda = 1.54178\,\text{Å}$) at a scanning speed of 0.02°/0.6 s. A FEG JEOL JSM 7600 field emission scanning electron microscope with an attached EDS detector was used to analyze the surface morphology and chemical composition of the samples. A FEG TEM Tecnai F20 microscope operating at 200 kV was used to analyze the structural characteristics of the crystallized samples. The analysis of the particle size was carried out in BIC 90 PLUS equipment. Nitrogen (N_2) adsorption-desorption isotherms were obtained using a Nova Touch LX1 (pore size and surface area analyzer).

3. Results

The X-ray diffraction pattern is shown in Figure 1. All XRD patterns for ZnO showed diffraction peaks corresponding to the (100), (002), (101), (102), (110), (103), (200), (112), (201), and (004) crystallographic planes and can be indexed to the Wurtzite hexagonal ZnO structure (ICSD#65119) belonging to the $P6_3mc$ space group. It can be seen that no peaks corresponding to any other materials or elements were observed in the samples. The strong broadening of diffraction lines for the ZnO nanopowders would be caused by the small size of the crystallites with imperfections within the crystalline lattice (stacking faults, vacancies, dislocations, and others). Similar results at synthesizing ZnO nanopowders by sol-gel route were determined by W L. de Almeida et al. [14]. Our results agree too with those obtained by Zi-Neng et al. [15], observing that when the temperature of the hydrothermal treatment increases, the ZnO microparticles present a preferential orientation in the *c*-axis, improving their crystallinity since the activation energy is adequate so that the atoms obtain more energy when the temperature increases. This allows the atoms with less surface energy to be transported to the best energy point of the crystal lattice, initiating the melting process in the crystallites, forming larger grains, and leading to the minimization of oxygen defects at the grain boundaries.

Figure 2 shows the micrographs of the scanning electron microscopy (SEM) analysis, in which agglomerated hexagonal microparticles with well-defined grain boundaries can be observed. V. Koutu et al. [16] noted that particle growth is determined by the concentration and subsequent reaction between the precipitating agent and the solution precursor.

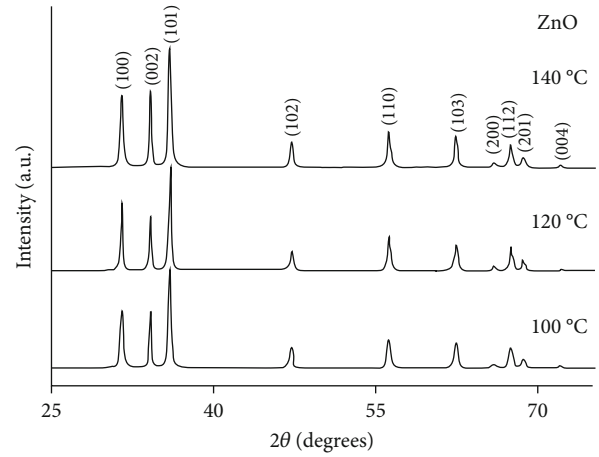

Figure 1: XRD patterns for mesoporous samples of ZnO in different temperatures, 100°C (AZN100), 120°C (AZN120), and 140°C (AZN140).

In our case, the molar ratio of reagent concentrations was 1 : 1, which leads us to think that the reaction of zinc acetate and sodium hydroxide in solution induces accelerated growth as the temperature of the hydrothermal treatment increases, as shown see in Figures 2(a)–2(c).

Along with this, the formation of mesopores in the ZnO microparticles is attributed to the following reactions:

$$\text{Zn}(\text{CH}_3\text{COO})_2 + 2\text{NaOH} \longrightarrow \text{Zn}(\text{OH})_2 + 2(\text{CH}_3\text{COO})\text{Na} \quad (1)$$

In Equation (1), the reaction between zinc acetate salt and sodium hydroxide is carried out by replacing elements in order to form zinc hydroxide (gel) and sodium acetate in the solution.

$$\text{Zn}(\text{OH})_2 + 2\text{H}_2\text{O} \longrightarrow \text{Zn}^{2+} + 2(\text{OH})^- + 2\text{H}_2\text{O} \quad (2)$$

$$\text{Zn}^{2+} + 2\text{OH}^- + 2\text{H}_2\text{O} \longrightarrow \text{Zn}(\text{OH})_4^{2-} + 2\text{H}^+ \quad (3)$$

In Equation (3), the Ostwald maturation process [14] is performed during the hydrothermal treatment, between the zinc hydroxide particles and the hydroxyl ions OH^-, to give rise to the hydroxylated species $\text{Zn}(\text{OH})_4^{2-}$.

$$\text{Zn}(\text{OH})_4^{2-} = \text{ZnO} + \text{H}_2\text{O} + 2(\text{OH})^- \quad (4)$$

Lastly, in Equation (4), the displacement of $(OH)^-$ free radicals is done so that the zinc oxide formation can occur.

The CH_3 and OH^- groups dissociate from each other, being transported out of the sample by distilled water during washing and by thermal decomposition after calcination, which opens a path for mesopores to form on the surface of ZnO particles, as seen in Figures 2(g)–2(i). Figures 2(d)–2(f) show the EDS spectra where only oxygen and zinc signals are detected, and the EDS map shows the uniform distribution of oxygen and zinc over the ZnO mesopores, as shown in Figures 2(g)–2(i).

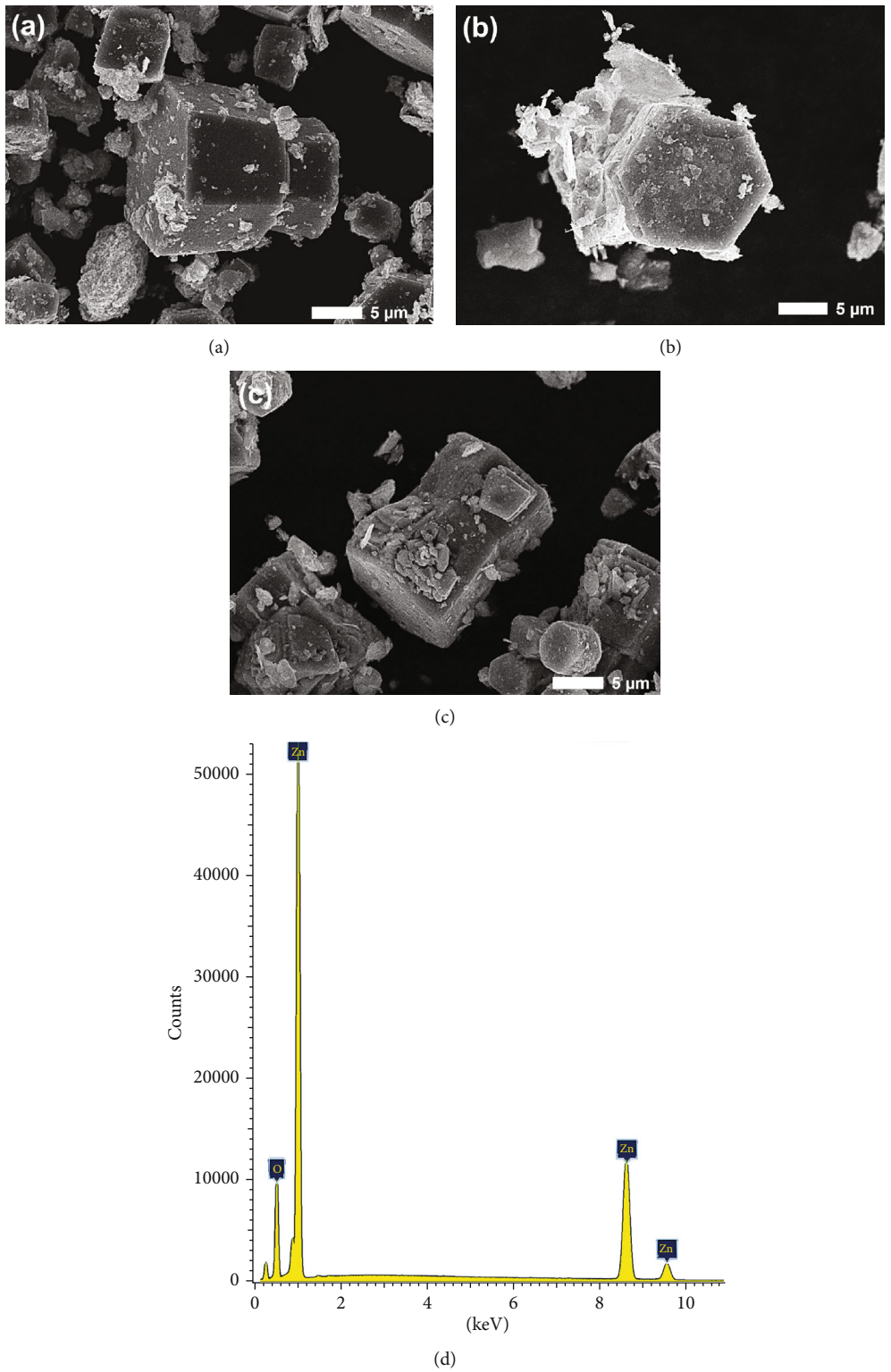

(a) (b) (c) (d)

Figure 2: Continued.

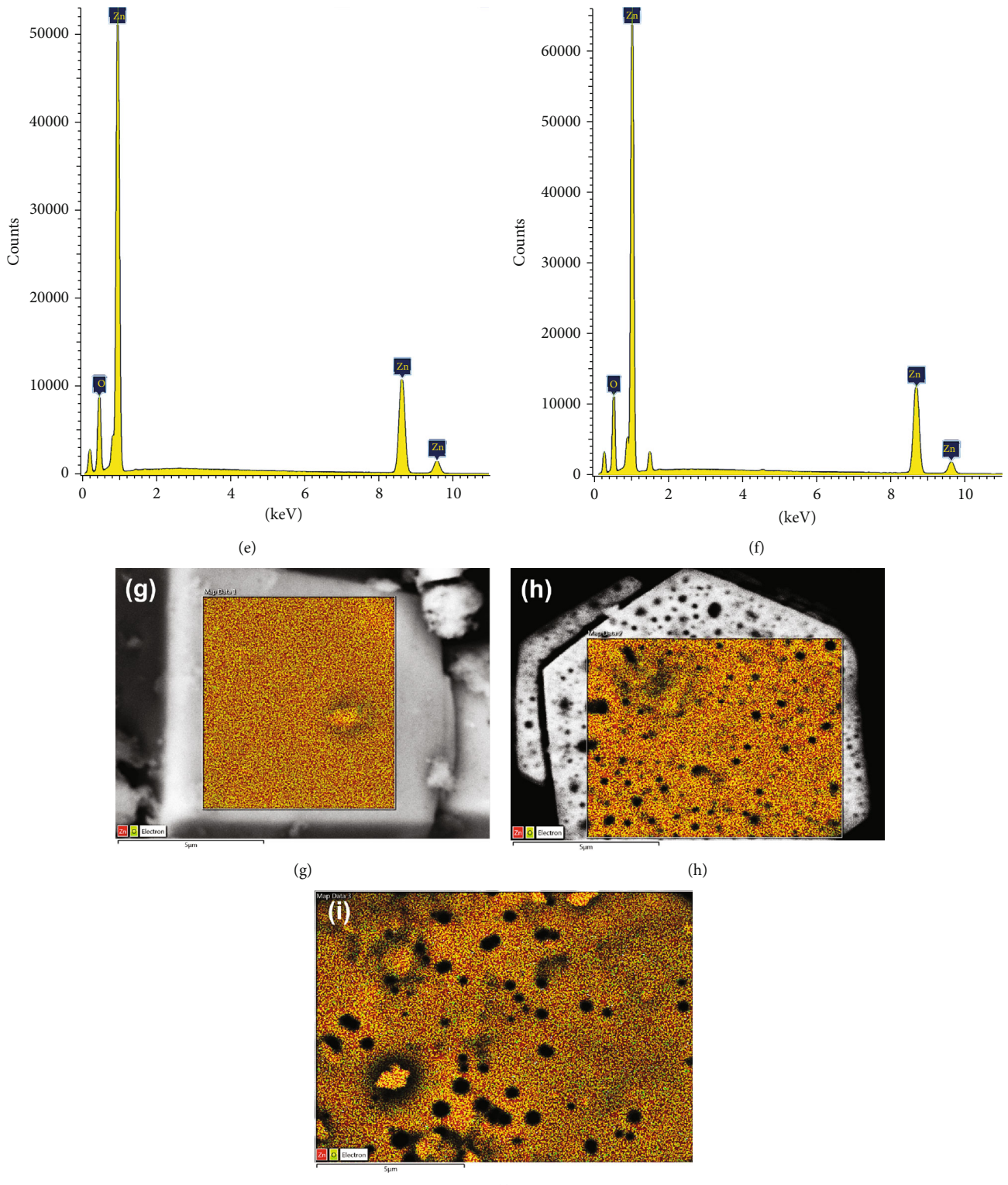

Figure 2: (a–c) FE-SEM images of ZnO microparticles, (d–f) EDS spectrum, and (g–i) EDS maps of mesoporous AZN100, AZN120, and AZN140 samples, respectively.

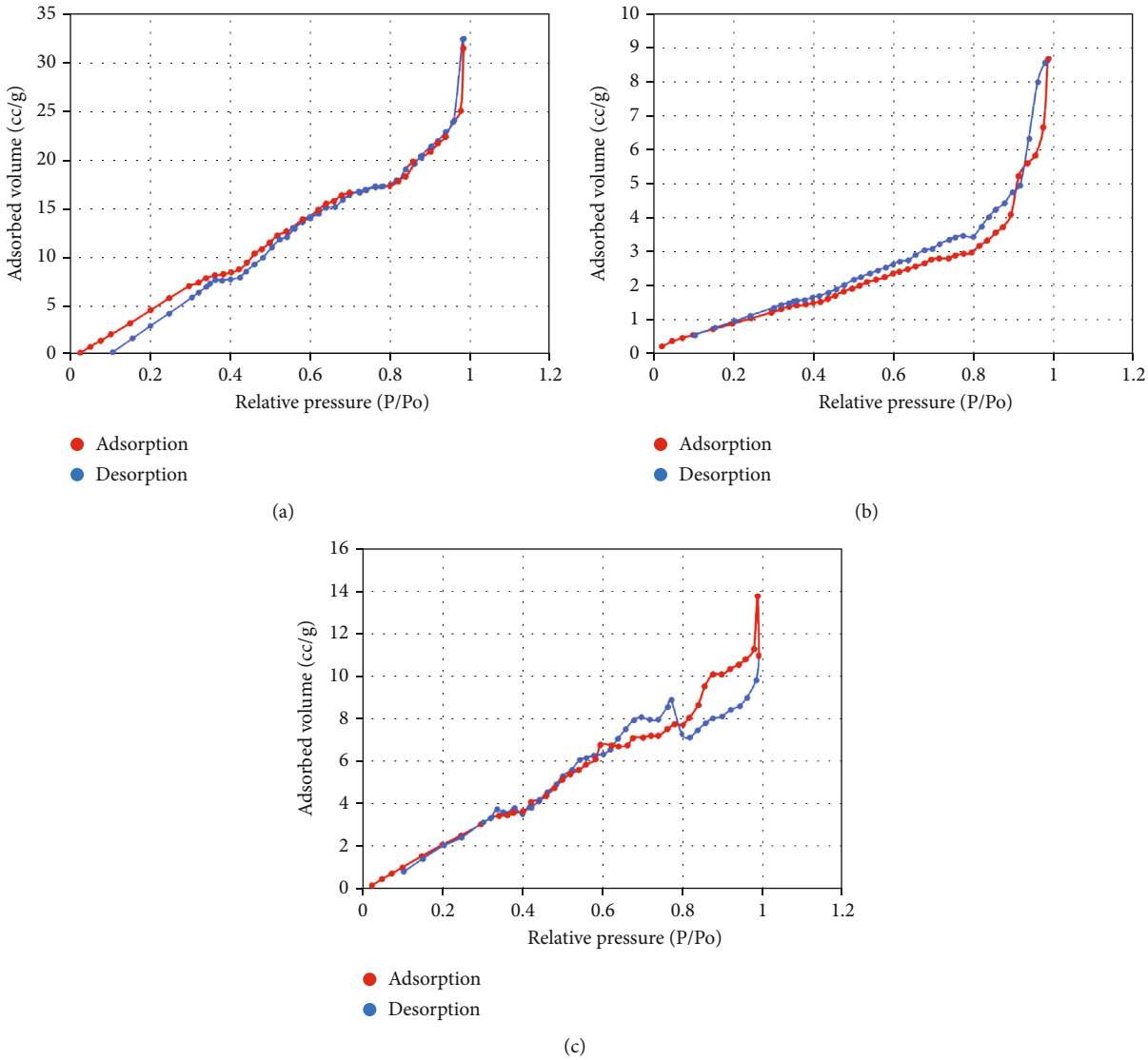

Figure 3: Physisorption isotherms of mesoporous ZnO: (a) AZN100, (b) AZN120, and (c) AZN 140.

Figure 3 shows that the desorption isotherm differs from the adsorption isotherm, in the relative pressure ($P/P0$) range of 0.30–0.99 for the mesoporous particles of the AZN100, AZN120, and AZN140 samples, respectively. The hysteresis can be explained by the connection and expansion of the pore size distribution that occurs within mesoporous materials.

According to results obtained by Yazhi Wang et al. [17] and V. Koutu et al. [16], the sol-gel method produced a homogeneous phase with micrometric grain size and a small increase in surface area, with a wide range of size distribution and pore volume, as can be seen in the enlarged image of Figure 2(h).

Table 1 shows the summary of the results obtained by BET analysis. The diameter of the pores is 3.4, 3.9, and 1.7 nm for the AZN100, AZN120, and AZN140 samples, respectively; on other hand, the size of the microparticles was 5 μm, which makes the mesopores of size and small volume. The temperature of the hydrothermal treatment directly influenced the formation of the mesopores, being the temperature of 120°C the one that presented the best results, and as can be seen in the enlarged image of Figure 2(h), such temperature promoted the distribution of the pore volume in the microparticles, as can be seen in the enlarged images of Figures 2(g)–2(i).

Table 1: Results obtained through BET analysis.

Sample	Surface area (m^2/g)	Pore diameter (nm)	Pore volume (cc/g)	Treatment temperature (°C)
AZN 100	40 ± 3	1.7 ± 0.1	0.01	100
AZN 120	4 ± 1	2 ± 0.1	0.01	120
AZN 140	21 ± 0.5	1.7 ± 0.1	0.01	140

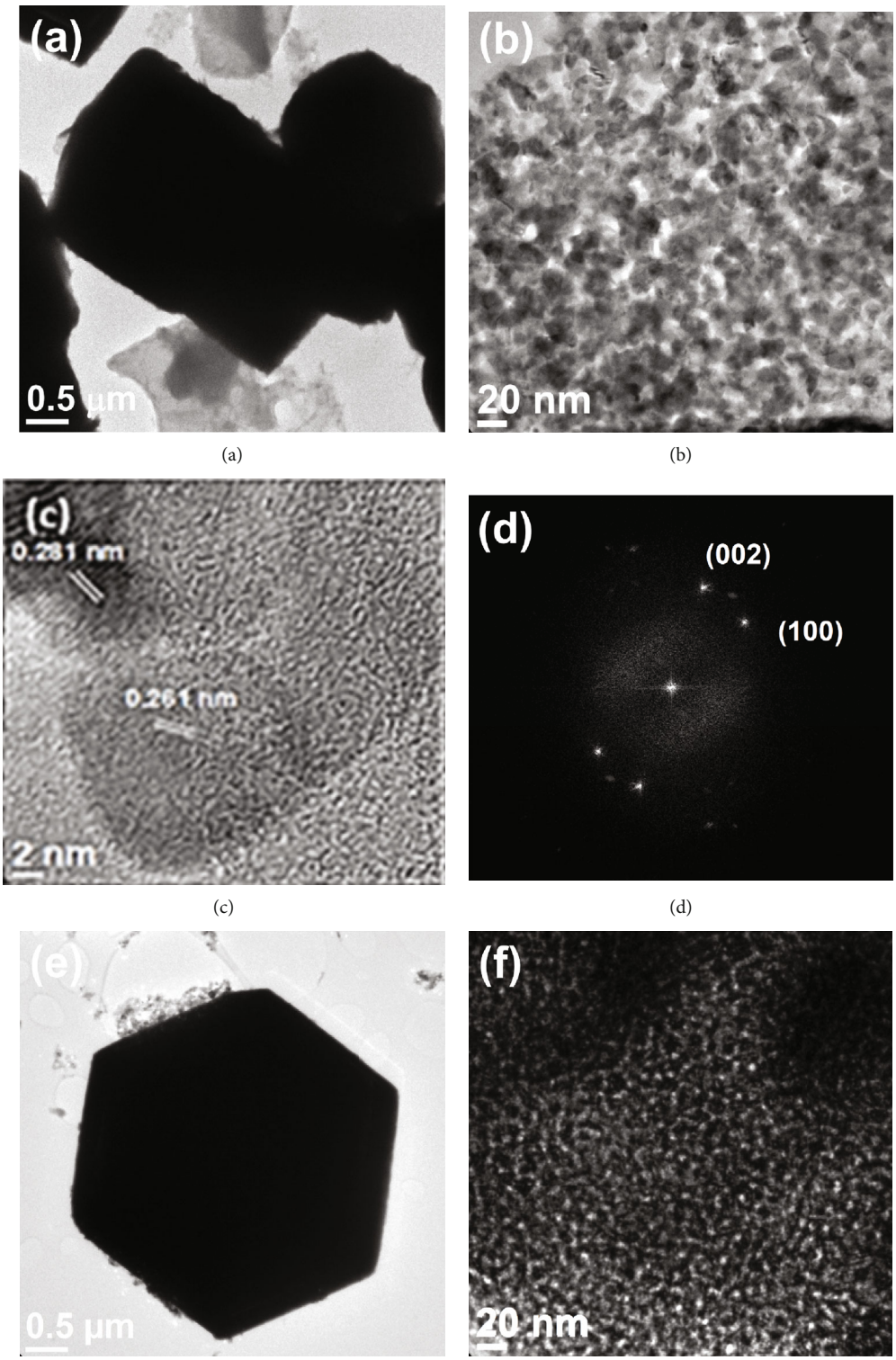

Figure 4: Continued.

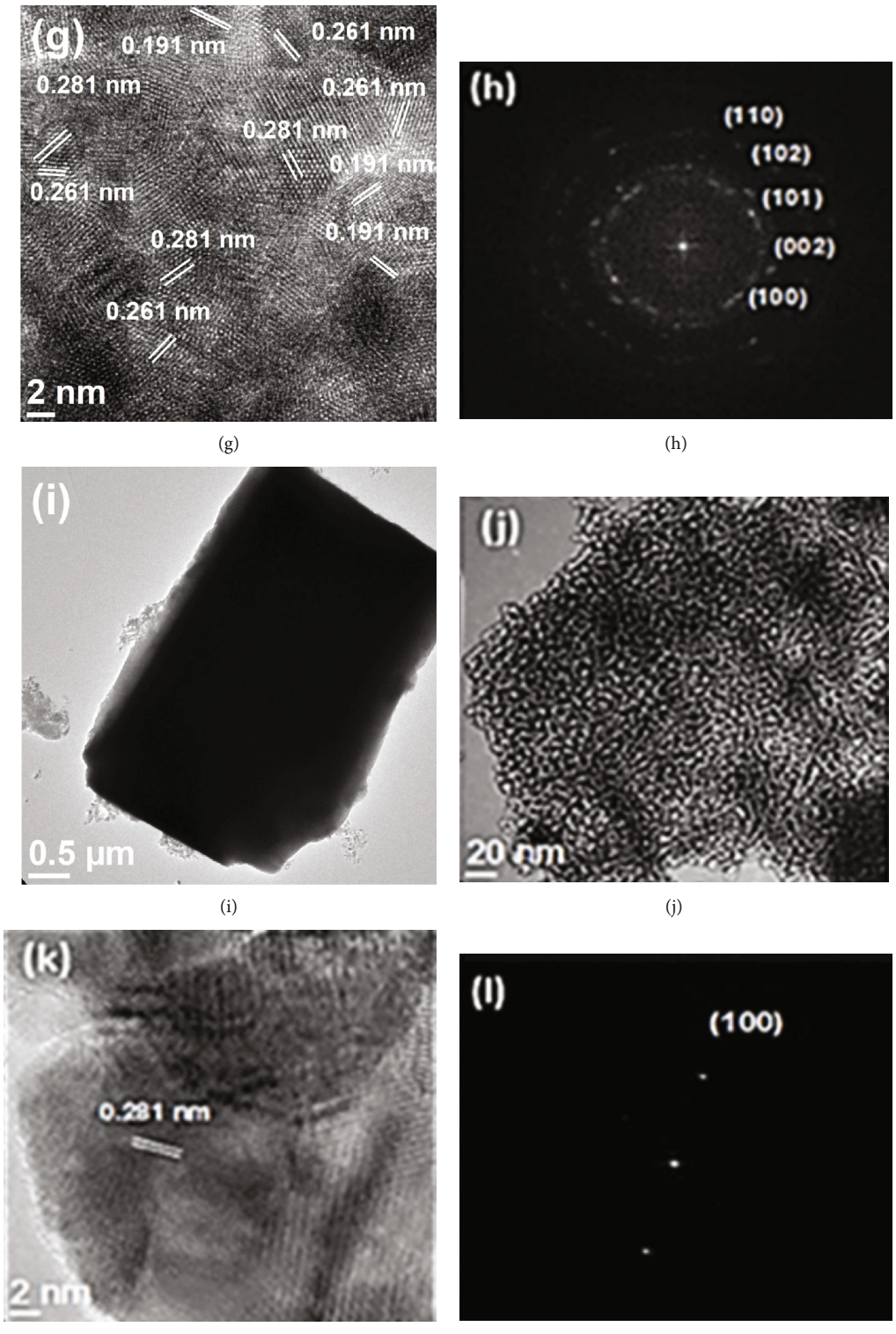

(g) (h)

(i) (j)

(k) (l)

Figure 4: (a, e, i) TEM images of the hexagonal ZnO matrix prism for AZN100, AZN120, and AZN140, respectively; (b, f, j) HRTEM images of mesoporous ZnO for AZN100, AZN120, and AZN140, respectively; (c, g, k) HRTEM images of mesoporous ZnO nanocrystals for AZN100, AZN120, and AZN140, respectively; (d, h, l) HRTEM FFT pattern images for AZN100, AZN120, and AZN140, respectively.

Figures 4(a), 4(e), and 4(i) show the top view of the transmission electron microscopy analysis of the AZN100, AZN120, and AZN140 samples, respectively. Figures 4(b), 4(f), and 4(j) show the mesoporous structure of the samples AZN100, AZN120, and AZN140, where the dark areas indicate the mesopores. The high-resolution transmission

electron microscopy image is shown in Figures 4(c), 4(g), and 4(k) for samples AZN100, AZN120, and AZN140. They show interatomic distances of 0.28 nm, 0.26 nm, and 0.19 nm that correspond to the crystallographic planes (1 0 0), (0 0 2), and (1 0 1) of ZnO. According to the work carried out by S. Bhattacharyya et al. [18], it is mentioned that the microstructure of ZnO is structurally uniform within itself, as observed in Figures 4(b), 4(f), and 4(j). It can also be seen that in Figures 4(d), 4(h), and 4(l), the FFT patterns show the characteristic planes of the wurtzite-type hexagonal structure.

4. Conclusions

Mesoporous ZnO microparticles were synthesized using the sol-gel method, with temperatures of 100°C, 120°C, and 140°C. No type of organic template was used for the formation of the mesopores, obtaining an increase in the surface area of the microparticles. The sample that shows the highest mesoporosity was the one synthesized at a hydrothermal treatment temperature of 140°C, with a surface area of 21 m [2]/g and a pore diameter of 1.7 nm. The influence of temperature was important because it internally modified the crystalline structure of the microparticles, in combination with the precursor, the precipitant, and the water. It was also corroborated that the hydrothermal treatment temperature causes an increase in the grain size, and the larger grains translate into a better crystallization of the sample. A simple, faster, ecological, and reproducible route for the synthesis of inexpensive mesoporous ZnO hexagonal microparticles and extend the method for the preparation of other materials.

Data Availability

The data used to support the findings of the study is included within the article.

Conflicts of Interest

The authors declare that they have no conflicts of interest.

Acknowledgments

The authors would like to thank CONACYT and CIC-UMSNH for providing their support.

References

[1] A. R. Marlinda, N. M. Huang, M. R. Muhamad et al., "Highly efficient preparation of ZnO nanorods decorated reduced graphene oxide nanocomposites," *Materials Letters*, vol. 80, pp. 9–12, 2012.

[2] C. Gu, J. Huang, Y. Wu, M. Zhai, Y. Sun, and J. Liu, "Preparation of porous flower-like ZnO nanostructures and their gas-sensing property," *Journal of Alloys and Compounds.*, vol. 509, no. 13, pp. 4499–4504, 2011.

[3] F. Xu, Y. Lu, L. Sun, and L. Zhi, "A novel ZnO nanostructure: rhombus-shaped ZnO nanorod array," *The Royal Society of Chemistry*, vol. 46, no. 18, pp. 3191–3193, 2010.

[4] M. H. Huang, S. Mao, H. Feick et al., "Room-temperature ultraviolet nanowire nanolasers," *Science*, vol. 292, no. 5523, pp. 1897–1899, 2001.

[5] Q. Li, H. Sun, M. Luo et al., "Room temperature synthesis of ZnO nanoflowers on Si substrate via seed-layer assisted solution route," *Journal of Alloys and Compounds.*, vol. 503, no. 2, pp. 514–518, 2010.

[6] S. Anandana, A. Vinu, N. Venkatachalam, B. Arabindoo, and V. Murugesan, "Photocatalytic activity of ZnO impregnated Hβ and mechanical mix of ZnO/Hβ in the degradation of monocrotophos in aqueous solution," *Journal of Molecular Catalysis A*, vol. 256, no. 1-2, pp. 312–320, 2006.

[7] V. C. Sousa, A. M. Segadães, M. R. Morelli, and R. H. G. A. Kiminamia, "Combustion synthesized ZnO powders for varistor ceramics," *International Journal of Inorganic Materials*, vol. 1, no. 3-4, pp. 235–241, 1999.

[8] X. Wang, F. Yang, W. Yang, and X. Yang, "A study on the antibacterial activity of one-dimensional ZnO nanowire arrays: effects of the orientation and plane surface," *Chemical Communications.*, vol. 42, no. 42, pp. 4419–4421, 2007.

[9] X. W. Lou, L. A. Archer, and Z. Yang, "Hollow micro-/nanostructures: synthesis and applications," *Advanced Materials*, vol. 20, no. 21, pp. 3987–4019, 2008.

[10] Q. Zhang, T. P. Chou, B. Russo, S. A. Jenekhe, and G. Cao, "Aggregation of ZnO nanocrystallites for high conversion efficiency in dye-sensitized solar cells," *Angewandte Chemie*, vol. 47, no. 13, pp. 2402–2406, 2008.

[11] A. Osinsky, J. W. Dong, M. Z. Kauser, B. Hertog, A. M. Dabiran, and P. P. Chow, "MgZnO/AlGaN heterostructure light-emitting diodes," *Applied Physics Letters*, vol. 85, no. 19, pp. 4272–4274, 2014.

[12] F. A. Lucca, A. Shigueaki, F. Severo, and C. Pérez, "Photocatalytic activity of nanoneedles, nanospheres, and polyhedral shaped ZnO powders in organic dye degradation processes," *Journal of Alloys and Compounds*, vol. 572, pp. 68–73, 2013.

[13] W. L. de Almeida, N. S. Ferreira, F. Severo, and V. Celdas, "Study of structural and optical properties of ZnO nanoparticles synthesized by an eco-friendly tapioca-assisted route," *Materials Chemistry and Physics*, vol. 258, article 123926, 2021.

[14] W. L. de Almeida, F. Severo, N. S. Ferreira, and V. Caldas, "Eco-friendly and cost-effective synthesis of ZnO nanopowders by Tapioca-assisted sol-gel route," *Ceramics International*, vol. 46, no. 8, pp. 10835–10842, 2020.

[15] Z. Neng, K. Y. Chan, and T. Tohsophon, "Effects of annealing temperature on ZnO and AZO films prepared by sol-gel technique," *Applied Surface Science*, vol. 258, no. 24, pp. 9604–9609, 2012.

[16] V. Koutu, L. Shastri, and M. M. Malik, "Effect of NaOH concentration on optical properties of zinc oxide nanoparticles," *Materials Science*, vol. 34, no. 4, pp. 819–827, 2016.

[17] Y. Wang, S. Zhu, X. Chen et al., "One-step template-free fabrication of mesoporous ZnO/TiO_2 hollow microspheres with enhanced photocatalytic activity," *Applied Surface Science.*, vol. 307, pp. 263–271, 2014.

[18] S. Bhattacharyya and A. Gedanken, "A template-free, sonochemical route to porous ZnO nano-disks," *Microporous and Mesoporous Materials.*, vol. 110, no. 2-3, pp. 553–559, 2008.